RADAR INTERFEROMETRY FOR GROUND SUBSIDENCE MONITORING USING ALOS PALSAR DATA

A.H. Ng[a,*], H. Chang[a], L. Ge[a], C. Rizos[a], M. Omura[b]

[a] Cooperative Research Centre for Spatial Information & School of Surveying and Spatial Information Systems, The University of New South Wales, Sydney NSW 2052, Australia – (alex.ng, hsing-chung.chang)@student.unsw.edu.au, (l.ge, c.rizos)@unsw.edu.au

[b] Department of Environmental Science, Kochi Women's University, 5-15 Eikokuji-cho, Kochi 780-8515, Japan - omura@cc.kochi-wu.ac.jp

Commission VII, WG VII/2

KEY WORDS: Remote Sensing, Land, Monitoring, SAR, Radar

ABSTRACT:

This paper describes the results using data from ALOS and ENVISAT satellites for the purpose of subsidence monitoring over underground coal mine sites in the state of New South Wales, Australia, using the differential interferometric synthetic aperture radar (DInSAR) technique. The quality of the mine subsidence monitoring results is mainly constrained by the noise due to the spatial and temporal decorrelation between the interferometric pair and the phase discontinuities in the interferogram. This paper reports on the analysis of the impact of these two factors on the performance of DInSAR for monitoring ground deformation. The ALOS L-band PALSAR DInSAR results have been compared to DInSAR results obtained from ENVISAT C-band ASAR data to investigate the performance of ALOS PALSAR for ground subsidence monitoring. Differential interferograms from SAR data acquired using different operating frequencies, for example, X-, C- and L-band, from the TerraSAR-X, ERS-1/2, ENVISAT, JERS-1 and ALOS satellite missions, were simulated. The simulation results showed that the new satellites ALOS, TerraSAR-X and COSMO-SkyMed perform much better than the others. ALOS PALSAR and ENVISAT ASAR images with similar temporal coverage were searched. The two-pass DInSAR technique with a 25m DEM was used to measure the location and amplitude of ground deformation. Strong phase discontinuities and decorrelation have been observed in almost all ENVISAT interferograms and hence it is not possible to generate the displacement maps. However these problems are minimal in ALOS PALSAR interferograms due to its spatial resolution and longer wavelength. Six successive subsidence maps are generated with eight ALOS PALSAR images from both ascending and descending orbits. The results are compared with ground survey data at two sites with RMS error of 1.7cm and 0.6cm being achieved. The accumulated subsidence can be estimated by adding up all subsidence maps; however the error in each DInSAR result, such as the geocoding error between each result, will also accumulate. An approach for minimising geocoding error in order to calculate the accumulated subsidence from a series of SAR images is described.

1. INTRODUCTION

1.1 Underground Mining in Australia

Ground subsidence is the lowering or collapse of the land surface which can be caused by either natural or anthropogenic activities. Most ground subsidence in Australia is human induced, and in non-urban areas is usually related to underground mining, especially for coal. The magnitude (areal extent and amount) of subsidence due to underground mining depends on a number of factors, including the depth of cover, overlying strata properties, seam thickness, panel width, chain pillar size and surface topography (Nesbitt, 2003). The rocks above the mine workings may not have adequate support and can collapse from their own weight either during mining or long after mining has been completed. Therefore ground subsidence due to underground mining is a major concern to the mining industry, government, environmental groups and others. In Australia most underground coal mines employ the longwall mining technique, where a long 'wall' of coal is mined in a single slice in order to maximise the recovery of coal. The subsidence caused by this technique can be very large, occur immediately after or during mining, and can therefore cause serious problems, for example, changing the river courses and damaging building foundations. The subsidence induced by this mining technique can have a spatial extent of several hundred metres.

Several methods are currently used for mine subsidence monitoring, including levelling, total station surveys, and GPS (Schofield, 1993). However these techniques have limitations, primarily because they measure subsidence on a point-by-point basis. Spaceborne differential radar interferometry (DInSAR) is a technique which can measure the ground movement (or deformation) of an entire area. It is quicker, less labour intensive and hence less expensive compared to the conventional ground-based survey methods.

1.2 Test Site

Two test sites were chosen for this study: Westcliff and Appin (Figure 1). The two underground mine sites are very close to each other and are therefore imaged in the same radar acquisition. The width of each longwall panel in the underground mines is about 200-300m, which is 100-150m from the edge to the centre of a longwall panel. The depth of the coalmines at these test sites is between 300-500m. The ground subsidence at the test sites have typical peak amplitudes

of 20 to 50cm about 1-2 months after the mine process has ceased, and can be up to 90-100cm over a full year.
As the peak subsidence at the mine site is much greater than the maximum subsidence that the European Space Agency satellite systems ERS SAR and ENVISAT ASAR can detect, the phase fringes in the ERS and ENVISAT interferogram corresponding to the ground surface displacement are expected to be saturated. One of the aims of this research was to investigate the capability of the Japanese ALOS PALSAR data for monitoring ground deformation caused by mining activities. The ALOS L-band PALSAR differential InSAR results have been compared to differential results obtained from other satellite SAR data such as ENVISAT C-band ASAR.

Figure 1. Location of the test sites (Appin & Westcliff) on a LANDSAT image.

2. METHODOLOGY

Spaceborne repeat-pass differential interferometric SAR (DInSAR) has already proven its value for ground deformation monitoring in many applications due to its high precision and high spatial resolution (Goldstein et al., 1993, Carnec et al., 1996, Ge et al., 2007, Chang et al., 2005). When the SAR system images the ground, both amplitude (strength) and phase (time) of the backscattered signals are recorded by the receiving antenna. By computing the phase difference from two SAR images acquired at different times it is possible to generate a radar interferogram, which contains information about the (static) topography and any displacement in the slant range direction that may have occurred between the two SAR image acquisition dates. However, the effect of atmospheric disturbance, orbit error and decorrelation noise should also be considered. Hence, the interferometric phase can be written as:

$$\Delta\phi = \phi_{Topo} + \phi_{Defo} + \phi_{Atmos} + \phi_{Orbit} + \phi_{Noise} \quad (1)$$

where $\Delta\phi$ = phase difference between the two images
ϕ_{Topo} = phase due to the topography
ϕ_{Defo} = phase due to the geometric displacement of the imaged point
ϕ_{Atmos} = phase due to atmospheric disturbance
ϕ_{Orbit} = phase due to orbit error
ϕ_{Noise} = phase due to decorrelation noise

In order to estimate the displacement all the other components should be carefully removed or accounted for. In this study, the topographic phase is removed using an independently derived digital elevation model (DEM). Since the spatial extent of subsidence is expected to be only of the order of several hundred metres, the atmospheric disturbance can be assumed insignificant (Carnec et al., 1996). The orbit error contribution can be corrected during DInSAR analysis, and the phase noise can be reduced by applying an adaptive filter. Therefore the phase due to geometric displacement of the point is given by (Zebker and Goldstein, 1986):

$$\Delta\phi_{defo} = \frac{4\pi}{\lambda}\Delta R \quad (2)$$

where λ = wavelength of the radar signal
acquisitions in the line-of-sight (LOS) direction

The displacement vector along the LOS of the radar system is a composite of the vertical, easting and northing displacement components. However, due to the lack of SAR data acquired from different viewing angles and orbit heading at a similar time period, it is not possible to derive the 3-D displacement vector. The deformation due to underground mining activity is most likely in the vertical direction, with the horizontal deformation being much smaller (Peng, 1986) and hence the horizontal displacement is assumed to be negligible for the purposes of this study. Under this assumption the LOS displacement can be converted into vertical displacement:

$$\Delta S = -\frac{\Delta R}{\cos(\theta_{inc})} \quad (3)$$

where ΔS = surface displacement in the vertical direction
θ_{inc} = incidence angle

3. SIMULATIONS

In order to avoid aliasing in phase-unwrapping process, the phase difference between any two adjacent pixels in the interferograms should be less than one-half cycle (π) (Chen et al., 2002), otherwise the wrapped phase in the interferogram becomes ambiguous and cannot be unwrapped. Therefore the maximum deformation of a whole subsidence bowl due to underground mining that can be detected without phase discontinuity can be written as:

$$S_{\max,LOS} = \frac{w}{g_{resolution}} \cdot \frac{\lambda}{4} \quad (4)$$

where $S_{max,LOS}$ = maximum deformation of the subsidence bowl in the LOS direction that can be detected without phase discontinuity
$g_{resolution}$ = ground resolution of the SAR sensor
w = radius of the subsidence bowl
$\lambda/4$ = distance corresponding to a one-half cycle of the interferometric phase

In the test sites, a subsidence bowl with radius of 150m is expected given that the width of each longwall panel is about 200-300m. Therefore, theoretically the expected maximum deformation that can be detected (without phase discontinuity) is approximately 8cm, 7cm, 48cm, 86cm, 39cm and 39cm for the wavelengths of the ERS, ENVISAT, JERS, ALOS, TerraSAR-X and COSMO SkyMed satellites respectively (assuming resolution of 25m, 30m 18m, 10m, 3m and 3m respectively), along the LOS direction.

A simulation is carried out to investigate this effect using a subsidence model (Figure 2) derived from an ALOS PALSAR DInSAR result. The model has a peak subsidence of 50cm. The subsidence model is rescaled based on the ground resolution of each satellite and is converted into absolute phase using equations (2) & (3). Differential interferograms are simulated by wrapping the absolute phase (Figures 2). The simulated differential interferograms are then converted back into LOS displacement by unwrapping the phase in the simulated differential interferogram using the MCF method (Costantini, 1998). The temporal and spatial decorrelation is not considered in this simulation. Phase saturation has been observed in both differential interferograms derived from ERS and ENVISAT data due to the high phase gradient in the subsidence model. In contrast, the phase fringes in the differential interferograms from ALOS, JERS, TerraSAR-X and COMOS SkyMed data are reasonably clear.

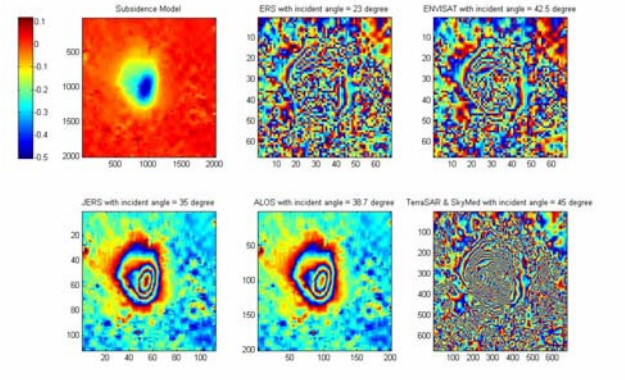

Figure 2. Simulated differential interferograms from various SAR satellites based on the subsidence model under noise-free conditions.

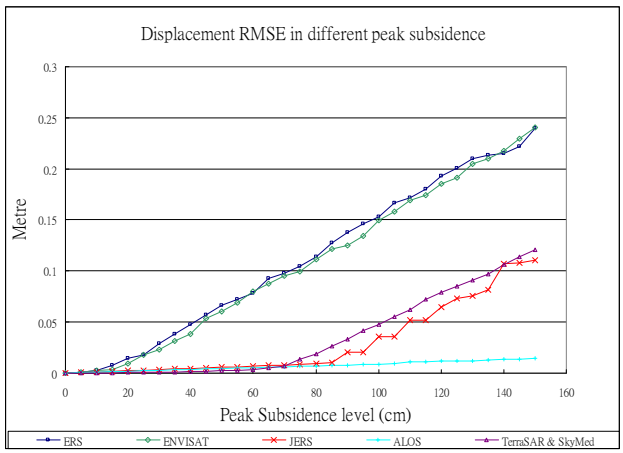

Figure 3. Detectable subsidence errors with different magnitudes of peak subsidence under noise-free conditions.

The simulation is repeated using a subsidence model with different peak subsidence (from 5cm to 150cm). The detectable subsidence errors (RMSE) with different peak subsidence are shown in Figures 3, which shows that the ALOS, TerraSAR-X and COSMO-SkyMed data are able to be used to measure larger displacement with much lower errors. The L-band ALOS PALSAR is able to maintain a low subsidence error with relatively high maximum detectable subsidence. High RMSE is observed in the ENVISAT and ERS results, with peak subsidence greater than 10cm.

4. RESULTS

ALOS and ENVISAT images with similar temporal coverage were searched for the test sites. The two-pass DInSAR technique with a 25m resolution DEM was used to estimate the location and amplitude of ground deformation. The performance of earlier SAR satellites ERS-1/2 and JERS-1 have already been discussed in a previous study (Ge et al., 2007).

4.1 ENVISAT ASAR

More than 90 ENVISAT images have been acquired over the same site during the period 07 July 2006 and 10 March 2008. The images were acquired from 7 different tracks, in both descending and ascending passes, with four different imaging modes. Although the location of the subsidence bowls can be identified from many ENVISAT differential interferograms, strong phase discontinuities and decorrelation have been observed in almost all ENVISAT interferograms, and hence it is not possible to generate displacement maps. Figure 4 shows an example of a differential interferogram generated using ENVISAT pairs for both mine sites. The interferogram derived from ENVISAT pairs show phase saturation near the centre of the subsidence bowl in the case of the Westcliff Mine, while the fringes at the rims of that subsidence bowl are reasonably clear. The phase of the interferogram in Figure 4 is unwrapped and is converted into vertical displacement. The maximum subsidence detected by the ENVISAT pair detected from the interferograms is about 5cm, whereas the expected subsidence is greater than 40cm. This is because the phases in the ENVISAT differential interferograms fail to correctly unwrapped due to phase saturation. The ENVISAT differential interferogram again shows phase saturation in the centre of the subsidence bowl in the case of the Appin Mine. Unlike the subsidence bowl in the Westcliff Mine, the fringes at the rim of the subsidence bowl in Appin are only clear in the upper parts of the image (low vegetation area) and are very noisy for the lower parts (heavily vegetated area). This suggested that ENVISAT images can be affected strongly by vegetation.

4.2 ALOS PALSAR

There are 10 ALOS PALSAR acquisitions available for the period from December 2006 to March 2008, from both ascending and descending passes, with two different imaging modes (FBS and FBD). Seven differential interferograms were generated based on the ALOS PALSAR images (Table 1). The ALOS PALSAR FBD data are oversampled by a factor of 2 in the range direction so that they can be co-registered with ALOS PALSAR FBS data for DInSAR processing. Figure 5 shows the differential interferograms generated by ALOS PALSAR pairs for a similar time period to the ENVISAT pairs (Figure 4). The fringes in the differential interferogram derived from the ALOS pair are very clear even at the centre of both subsidence bowls.

It is important to note that the fringes are very clear in the heavily vegetated area, and the phase can still be unwrapped correctly. A maximum subsidence of approximately 40cm has been measured at the Appin Mine site between the period 29 Jun 2007~14 Aug 2007. It is observed that the phase discontinuities and decorrelation problems are much less in the case of the ALOS PALSAR interferograms compared to the ENVISAT ASAR interferograms, which is mainly due to the fact that ALOS PALSAR images have finer spatial resolution and longer wavelength. Because of these factors ALOS PALSAR has much higher successful rate for generating displacement maps, especially for pairs with difference of only 1 repeat cycle. With this advantage, six successive subsidence maps were able to be generated with eight ALOS PALSAR images from both ascending and descending orbit acquisitions. The 6 DInSAR results generated from interferograms 2-7 (Table 1) are post-processed and overlaid on the mine plan in Figure 6. The location has been confirmed by comparison with the actual mine schedule.

Interferogram	Pair 1		Pair 2		Oribit Heading	Period (Days)	Perpendicular Baseline (m)
	Date	Mode	Date	Mode			
1	27 Dec 2006	FBS	11 Feb 2007	FBS	Ascending	46	530
2	29 Jun 2007	FBD	14 Aug 2007	FBD	Ascending	46	45
3	14 Aug 2007	FBD	29 Sep 2007	FBD	Ascending	46	-501
4	29 Sep 2007	FBD	14 Nov 2007	FBS	Ascending	46	-110
5	14 Nov 2007	FBS	30 Dec 2007	FBS	Ascending	46	-735
6	30 Dec 2007	FBS	14 Feb 2008	FBS	Ascending	46	24
7	06 Feb 2008	FBS	23 Mar 2008	FBS	Descending	46	-127

Table 1. ALOS PALSAR interferogram data used for this study.

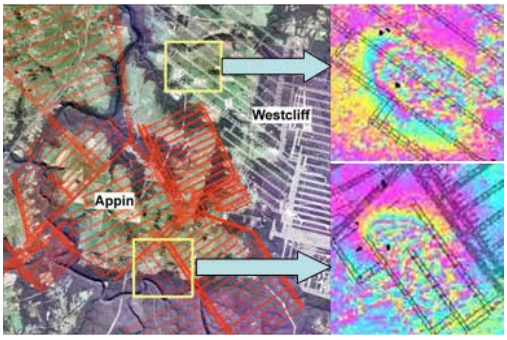

Figure 4. (Left) Mine plan overlaid with high resolution optical image. (Right) ENVISAT ASAR differential interferogram acquisition during 05 Jul 2007~09 Aug 2007 (35 days) with Bperp (perpendicular baseline) = 89.94m, ascending pass, IS1 on (upper right) Westcliff Mine and (lower right) Appin Mine.

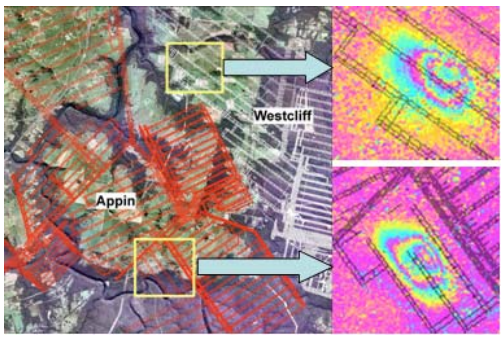

Figure 5. (Left) Mine plan overlaid with high resolution optical image. (Right) ALOS PALSAR differential interferogram acquisition during 29 Jun 2007~14 Aug 2007 (46 days) with Bperp = 44.75m, ascending pass, on (upper right) Westcliff Mine and (lower right) Appin Mine.

4.3 Validation

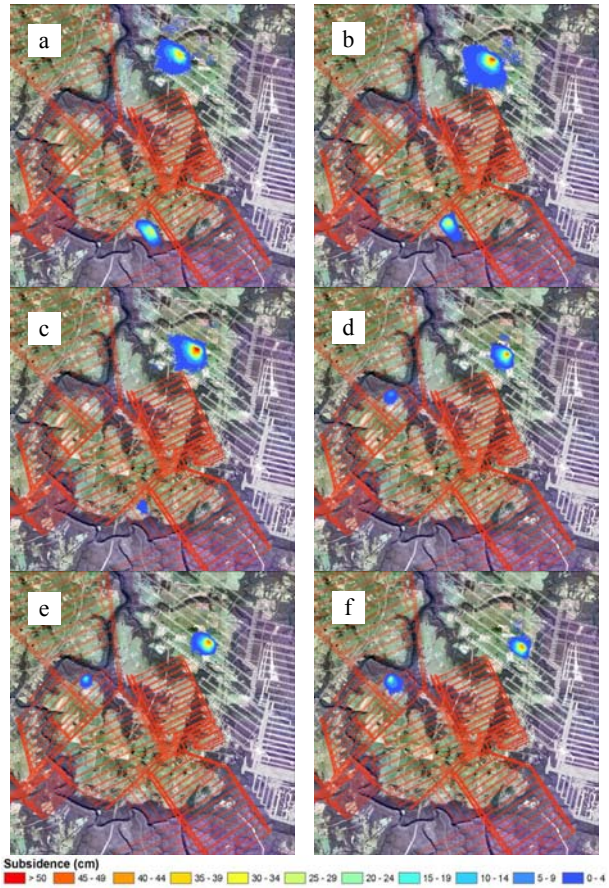

Figure 6. Colour-coded DInSAR-derived subsidence maps from ALOS PALSAR data pairs from (a) 29 Jun 2007~14 Aug 2007, (b) 14 Aug 2007~29 Sep 2007, (c) 29 Sep 2007~14 Nov 2007, (d) 14 Nov 2007~30 Dec 2007, (e) 30 Dec 2007~14 Feb 2008, (f) 06 Feb 2008~23 Mar 2008. Positive displacement indicates subsidence.

To validate the results obtained, the ALOS PALSAR DInSAR results are compared against ground survey data for both mine sites. The DInSAR subsidence profile extracted from the ground survey points (Figure 7), compared with the ground survey data measured on 19 September 2007 and 12 November 2007 at the Westcliff Mine, is shown in Figure 8. Figure 8 shows that the DInSAR result matchs well with the ground survey data. The subsidence profile along point LO01 – LO21 has an RMSE of 0.6cm. The result suggests that this DInSAR technique has the capability to deliver sub-centimetre accuracy.

Figure 9 shows the DInSAR height change result from ALOS images acquired on 27 Dec 2006 and 11 Feb 2007 and overlaid on Appin Mine plan and ground survey points (N042-N142). In order to assess the quality of the DInSAR result it is important to have good spatial and temporal overlap between the DInSAR result and the ground survey data. Unfortunately the difference between the date of the ground survey and the two ALOS PALSAR image acquisitions is quite significant in the case of Appin. The closest ground survey dates before and after the two acquisitions are in 19 Oct 2006 and 15 Jan 2007 for ALOS images 27 Dec 2006 and 06 Feb 2007 and 20 Feb 2007 for ALOS images 11 Feb 2007. In order to compare the ground survey data with DInSAR result, the deformation is assumed to change linearly between the ground survey dates before and after each ALOS acquisitions. The estimated height at 27 Dec 2006 (estimated from 19 Oct 2006 and 15 Jan 2007) is then subtracted from the estimated height at 11 Feb 2007 (estimated from 06 Feb 2007 and 20 Feb 2007) and the comparison to the DInSAR result is shown in Figure 10. It can be seen that the DInSAR result and the ground survey data agree well with most survey points, including the area with the highest rate of subsidence. However, most of the error has been found from survey point number N80-N105, which is at the east of the subsidence bowl. Up to 4cm difference has been observed from point N80-N84. Apart from these points, the DInSAR result follows the ground truth very well and an RMSE of 1.7cm has been calculated.

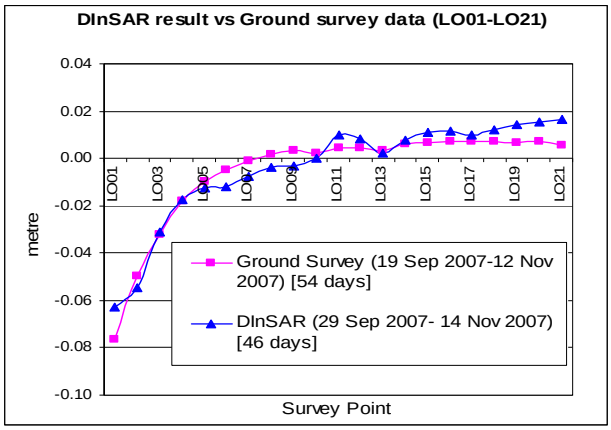

Figure 8. Validation of DInSAR-derived subsidence profiles against ground truth.

It is interesting to note that the subsidence bowl from the displacement maps derived from ascending (Figure 6e) and descending (Figure 6f) pairs are slightly different. For the ascending pairs (Figure 6a-e), the subsidence bowl seems to have higher subsidence in the west, whereas the subsidence bowl seems to have higher subsidence in the east for the descending pair (Figure 6f). This maybe caused by different displacements vector and incidence angle between two tracks. This may explain why the most of the error has been found on the east of the subsidence bowl.

The RMSE 0.6cm and 1.7cm between the DInSAR-derived results and ground survey data have been observed in the two sites. The inconsistency between the ground survey data and the DInSAR result can be due to several reasons: (1) difference between the date of survey and the date of satellite image acquisitions, (2) the uncertainties in the georeferencing, (3) errors in the DInSAR processing, and (4) errors in the ground surveys.

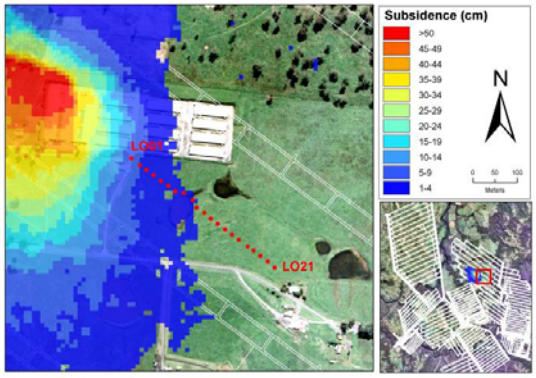

Figure 7. DInSAR height change derived from ascending ALOS images acquired on 29 Sep 2007 and 14 Nov 2007 (46 days apart) and overlaid on Westcliff Mine plan.

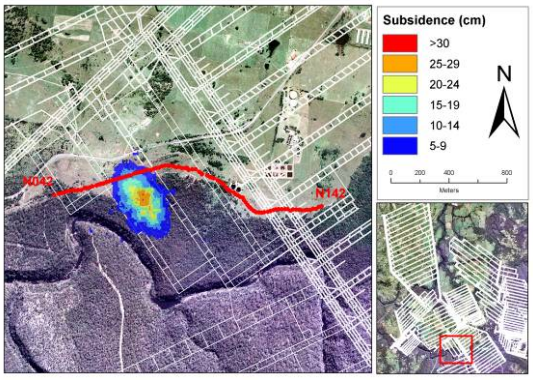

Figure 9. DInSAR height change derived from ascending ALOS images acquired on 27 Dec 2006 and 11 Feb 2007 (46 days apart) and overlaid on Appin Mine plan.

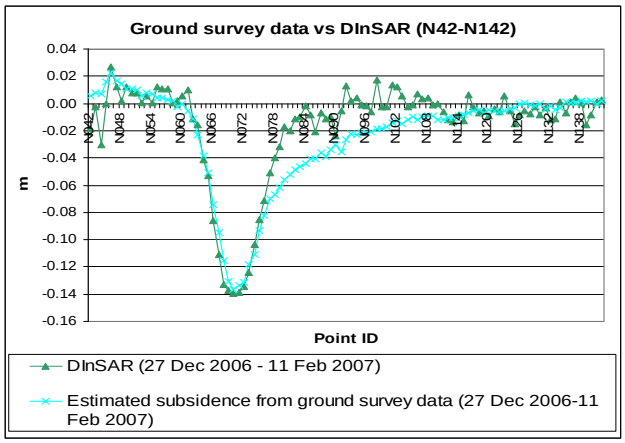

Figure 10. Validation of DInSAR-derived subsidence profiles against ground truth.

4.4 Accumulated Subsidence

The accumulated subsidence has been derived for the period 29 Jun 2007 to 14 Feb 2008 (230 days) using the 6 ascending ALOS PALSAR images (Figure 11). In the most ideal situation, the height displacement between 29 Jun 2007 and 14 Feb 2008 should be directly calculable from the differential interferogram 29 Jun 2007~14 Feb 2008. However, similar to other differential interferograms over long time spans, it is usually very difficult to unwrap the interferometric phase correctly due to high deformation gradient and decorrelation. Therefore an alternative technique was used to compute the subsidence for the period 29 Jun 2007~14 Feb 2008 by accumulating the subsidence from successive SAR pairs. The simplest way to determine the accumulated subsidence is to combine all subsidence maps generated from each ALOS pairs. However, the error in each DInSAR result will also be accumulated.

In order to reduce the geocoding error between each DInSAR result and the noise due to accumulating the deformation, a simple approach has been developed, as outlined below. (1) All ALOS PALSAR images were first resampled with respect to a reference master. (2) DInSAR analysis was then carried out to measure the deformation of the same points in each co-registrated images, i.e. interferograms 2-6 in this study (Table 1). (3) The deformations calculated from the five differential interferograms were added together (in slant range) prior to geocoding the accumulated deformation map. (4) Geocode the accumulated deformation map. Given the assumption that the expectation of the atmospheric delay for a point in k acquisitions is 0 (Kampes et al., 2006), the atmospheric noise would also be reduced by this method. The descending pair is not included in the accumulated subsidence map because the descending image may measure different scattering objects to the ascending image for the same pixel. Hence the deformation measured from the descending pair may not be consistent with the ascending pair if their deformation values are accumulated. Horizontal deformation which causes inconsistencies between ascending pair and descending pair is another issue which needs to be considered.

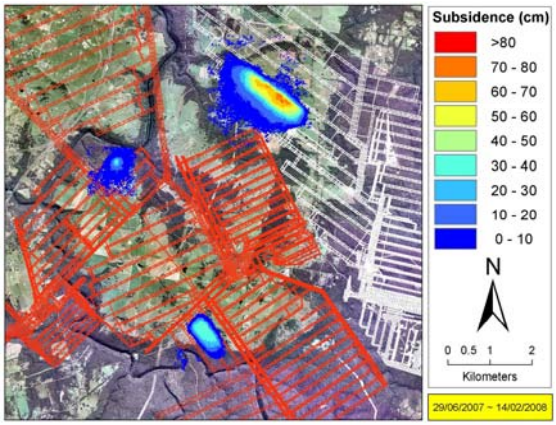

Figure 11. Accumulated subsidence of all subsidence maps for the period 29 Jun 2007 ~ 14 Feb 2008 (230 days).

5. CONCLUDING REMARKS

This study illustrated the capability of ALOS PALSAR for mine subsidence monitoring in Australia. Simulations have shown that the new satellites ALOS, TerraSAR-X and COSMO-SkyMed perform much better than the satellites launched before 2006 for this monitoring application. Differential interferograms from ALOS PALSAR and ENVISAT ASAR images with similar temporal coverage were generated. Strong phase discontinuities and decorrelation have been observed in almost all ENVISAT interferograms, whereas these issues are almost invisible in ALOS PALSAR interferograms due to its better spatial resolution and longer wavelength. Six successive subsidence maps derived from eight ALOS PALSAR images using both ascending and descending passes were obtained. More than 50cm subsidence has been found in the Westcliff Mine over 46 days. The DInSAR results derived from ALOS PALSAR data were validated with ground survey data at both mine sites. RMSE of 1.7cm and 0.6cm has been found in the Appin and Westcliff mine areas respectively. This study demonstrated an easy to implement approach to calculating the accumulated subsidence from a series of SAR images by resampling a series of SAR images into a reference master. This approach could minimise geocoding error between each DInSAR result and the error due to accumulating the results over several DInSAR results.

ACKNOWLEDGEMENTS

This research work has been supported by the Cooperative Research Centre for Spatial Information through Project 4.09, whose activities are funded by the Australian Commonwealth's Cooperative Research Centres Programme. The Australian Research Council has been supporting DInSAR research at UNSW over a number of years. The Australian Coal Association Research Program has also supported research for ground subsidence monitoring using DInSAR. The authors wish to thank the European Space Agency and the Earth Remote Sensing Data Analysis Center (ERSDAC) for providing the ENVISAT ASAR and ALOS PALSAR data, respectively. METI and JAXA retain ownership of the ALOS PALSAR original data. The PALSAR L-1.1 products were produced and distributed to the IAG Consortium for Mining Subsidence Monitoring. The authors also wish to thank BHP-Billiton for providing the ground survey data and other spatial data.

REFERENCES

Carnec, C., D. Massonnet and C. King, 1996. Two examples of the use of SAR interferometry on displacement fields of small spatial extent. *Geophysical Research Letters*, **23(24)**, 3579-3582.

Chen, C.W. and H.A. Zebker, 2002. Phase unwrapping for large SAR interferograms: statistical segmentation and generalized network models. *Geoscience and RemoteSensing, IEEE Transactions,* **40(8)**, 1709-1719.

Chang, H.C., L. Ge and C. Rizos, 2005. Radar interferometry for monitoring land subsidence due to underground water extraction. *Spatial Sciences Conference*, Melbourne, Australia, 12-16 September, pp. 736-743, CD-ROM procs.

Costantini, M., 1998. A novel phase unwrapping method based on network programming. *Geoscience and Remote Sensing, IEEE Transactions,* **36**, 813-818.

Ge, L., H.C. Chang and C. Rizos, 2007. Mine subsidence monitoring using multi-source satellite SAR images. *Journal of Photogrammetric Eng. & Remote Sensing*, **73(3)**, 259-266.

Goldstein, R.M., H. Engelhardt, B. Kamb and R.M. Frolich, 1993. Satellite radar interferometry for monitoring ice sheet motion: Application to an Antarctic ice stream, *Science*, **262**, 1525 – 1530.

Kampes, B. M., 2006. *Radra Interferometry : Persistent Scatterer Technique*. Springer, 22-23.

Nestbitt, A., 2003. Subsidence Monitoring West Cliff Colliery Longwall 5A4, *APAS (Association of Public Authority Surveyors) 2003 Conference*, Wollongong, Australia, 1-4 April, 133-139

Peng, S., 1986. *Coal Mine Ground Control*, 2nd Edition, John Wiley & Sons, 506pp.

Schofield, W., 1993. *Engineering Surveying*, Laxton's, Oxford, UK, 554pp.

Zebker, H.A. and R.M. Goldstein, 1986. Topographic mapping from interferometric synthetic aperture radar observations. *J. Geophys. Res.*, **91(B5)**, 4993-4999.